



# CO<sub>2</sub> microbubble colloidal gas aphrons for EOR application: the generation using porous filter, diameter size analysis and gas blocking impact on sweep efficiency

Mochammad Andy Natawijaya<sup>1,2</sup> · Yuichi Sugai<sup>1</sup> · Ferian Anggara<sup>2,3</sup>

Received: 22 March 2019 / Accepted: 6 May 2019 / Published online: 13 May 2019  
© The Author(s) 2019

## Abstract

The CO<sub>2</sub> is regarded to be an excellent solvent for miscible flooding. However, it is still facing a main problem which is the high mobility. Microbubbles with their unique characters offer some advantages for CO<sub>2</sub> EOR application. Different pore throat size filters were used to generate different dominant sizes of microbubbles that were injected into sandpicks under tertiary condition. Microscopic analysis was carried out to visualize the presence, stability and behavior of microbubbles inside the solution and porous media. The microbubbles with a dominant size of 10–50 μm showed additional 26.38% of oil recovery, showing their advantages over a larger dominant size of microbubbles up to 5.28% of oil recovery. The injection with larger microbubbles with a dominant size of 70–150 μm showed 27.5% of higher injection pressure than with a smaller dominant size of microbubbles, showing their advantage in gas blocking ability. In the heterogeneous porous media experiment, the recovery volume ratio between low- and high-permeability sandpicks was increased from 1:57 during water flooding to 1:4 during the CO<sub>2</sub> microbubble injection with 74.65% of additional recovery from a low-permeability zone, showing the microbubble gas blocking capability to change the flow pattern inside heterogeneous porous media.

**Keywords** CO<sub>2</sub> EOR · Microbubble · Colloidal gas aphrons · Tertiary recovery

## Introduction

Improved oil recovery can be done by injecting CO<sub>2</sub> to recover some of the remaining oil inside reservoir (Blunt et al. 1993). In general, additional 8–16% of original oil in place can be improved by such tertiary recovery (Rogers and Grigg 2000). CO<sub>2</sub> is an excellent solvent for miscible CO<sub>2</sub> flooding, and it can extract heavier components up to C<sub>30</sub>, reduces oil viscosity and reduces the surface tension of oil

and water that will improve the oil displacement (Stalkup Jr 1978). Despite those advantages, the CO<sub>2</sub> injection for EOR application is still facing some drawbacks; one of them is the high mobility of the CO<sub>2</sub> (Holm and Josenl 1974). The high gas mobility, in addition to reservoir heterogeneity and gravity segregation, often caused early gas breakthrough and less sweep efficiency (Lake 1989). Several attempts have been made to overcome this problem, such as alternating the injection between the water and CO<sub>2</sub> (WAG) and adding some foaming solutions during the CO<sub>2</sub> injection (Ghedan 2009). The nonylphenol ethoxylate sulfonate (NPES), a newly synthesized CO<sub>2</sub> philic surfactant, has also been reported to have a great potential in CO<sub>2</sub> EOR applications for reducing the interfacial tension and CO<sub>2</sub> mobility (Sagir et al. 2016). A recent study on surfactant-alternating gas/CO<sub>2</sub> (SAG) and alkaline surfactant-alternating gas/CO<sub>2</sub> (ASAG) shows a better recovery results than that of WAG (Phukan et al. 2019).

The success application of microbubble in drilling muds for sealing the formation to reduce/stop the losses during drilling operation and dealing with depleted reservoir initiate the application of microbubble for the EOR application.

✉ Mochammad Andy Natawijaya  
mochammad.andy.natawijaya@mail.ugm.ac.id

<sup>1</sup> Resources Production and Safety Engineering Laboratory, Department of Earth Resources Engineering, Faculty of Engineering, Kyushu University, 744 Matooka, Nishi-ku, Fukuoka 819-0395, Japan

<sup>2</sup> Department of Geological Engineering, Faculty of Engineering, Universitas Gadjah Mada, Jl. Grafika No. 2, Yogyakarta 55281, Indonesia

<sup>3</sup> Unconventional Geo-resources Research Center, Faculty of Engineering, Universitas Gadjah Mada, Jl. Grafika No. 2, Yogyakarta 55281, Indonesia

A micro-environment that separated the bulk fluid from formation was established by microbubble entering the formation (Growcock 2005). The resistance of microbubbles was increased simultaneously with the microbubble volume injected into porous media, and this showed the microbubble effective blocking ability (Bjorndalen et al. 2011). Under X-ray CT system observation, CO<sub>2</sub> microbubble flow spread evenly than normal CO<sub>2</sub> gas, especially in vertical direction within the core sample (Akai et al. 2015). These unique characters of microbubbles will be able to increase the EOR recovery by improving the sweep efficiency area and driving the fluid flow pattern during EOR injection from flowing dominantly in high-permeability to lower-permeability zone (Fig. 1a).

The microbubble colloidal gas aphron (MB-CGA) is a stabilized bubble with a diameter approximately 10–100 μm suspended in bulk liquid and consists of three layers (Sebba 1987). The inner layer is made of surfactant molecules encapsulating the gas core. The middle layer is a mixture of viscous water, stabilizer agent (polymer) and surfactant molecules that provide hydrophilic layer inward and outward. The outer layer consists of surfactant molecules that provide hydrophobic outward boundary (Fig. 1b, c).

The unique structure of MB-CGA will allow the bubble to agglomerate without coalescence. The stability of the agglomerated aphrons could reach a period of months (Gupta and Cawiezel 2013), and they could hold their stability under pressurization of 20.7 MPa (Growcock 2005). Other specific study on CO<sub>2</sub> microbubble stabilization showed that CO<sub>2</sub> MB-CGA can survive at a pressure of 13.8 MPa and a temperature of 50 °C (Telmadarreie et al. 2016).

Previous studies on MB-CGA were focused on analyzing the microbubble rheology and stability under different concentrations of surfactant and polymer and different temperature and pressure conditions (Longe 1989; Growcock 2005; Bjorndalen et al. 2011; Gupta and Cawiezel 2013). The MB-CGA was also found to improve the oil recovery

with tertiary condition which increased by 26.8% compared with 20.3% recovery by polymer injection (Shi et al. 2016).

Specific studies focusing on CO<sub>2</sub> MB-CGA were also investigated for the characterizations and flow behavior of porous media. Base fluid for CO<sub>2</sub> MB-CGA generation with good stability and viscosity was obtained by a mixing of 0.29 wt.% Surfonic N-85 surfactant with 0.55 wt% of xanthan gum polymer (Ghosh 2013). CO<sub>2</sub> MB-CGA showed higher injectivity compared with the base fluid even though both fluids almost have the same recovery up to 98% (Telmadarreie et al. 2016).

There were also studies on CO<sub>2</sub> microbubbles generation without using surfactant and polymer solution, and the structure of these bubbles was different with the previously mentioned MB-CGA. The bubbles in the size of micron were generated by injecting supercritical CO<sub>2</sub> through microporous filter into saline fluid under a pressure of 10 MPa and a temperature of 40 °C, and pore-size distribution in a filter was an important factor when generating CO<sub>2</sub> microbubbles (Xue et al. 2011). The experiment with these microbubbles under secondary recovery core flooding showed an increase of 13% of oil recovery compared with normal CO<sub>2</sub> injection (Akai et al. 2015). The same study was carried out under tertiary recovery, and the result also showed the same, additional oil recovery of 13% (Hiramoto et al. 2016).

CO<sub>2</sub> microbubbles with their unique characters offer some advantages for the EOR application. Since microbubbles contain a wide range of size distributions up to 200 μm at an initial time after generation (Telmadarreie et al. 2016), it will be very interesting to find out their diameter size effects to the sweep efficiency in EOR application. Unlike other authors who used high-speed steering for CO<sub>2</sub> MB-CGA generation in their experiments, this study used special porous filter for the CO<sub>2</sub> MB-CGA generation. Different pore throat size filters was used to create different dominant sizes of CO<sub>2</sub> MB-CGA. Gas blocking ability analysis and microbubble diameter size impact on

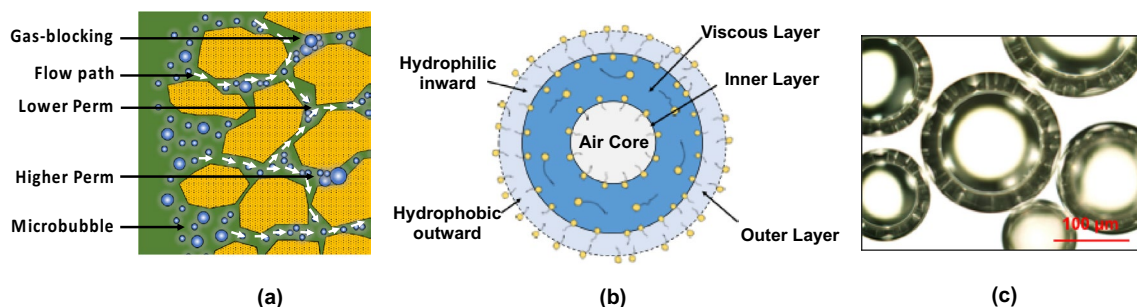


**Fig. 1** a Illustration of microbubble gas blocking ability, b microbubble colloidal gas aphrons structure, c microscopic image of CO<sub>2</sub> MB-CGA generated using a porous filter

sweep efficiency was carried out in tertiary recovery conditions on a laboratory sandpack experiments.

## Experimental procedure

### Materials and methods

The xanthan gum polymer ( $C_{35}H_{49}O_{29}$ ) provided by Junsei Chemical Co. Ltd., Japan, was used for stabilization of  $CO_2$  MB-CGA. Polymer is an essential component for enhancing the stability of microbubbles. It increases the viscosity of water in the middle layer of MB-CGA structure. The sodium dodecyl sulfate anionic surfactant ( $C_{12}H_{25}NaO_4S$ ) provided by Tokyo Chemical Co. Ltd., Japan, was used to reduce the interfacial tension. The solution was prepared by mixing of 0.4 wt.% of xanthan gum and 0.3 wt.% of sodium dodecyl sulfate with tap water. The GF-300 digital scale provided by A&D Company Ltd., Japan, was used to weigh the polymer and surfactant powder. The MS-H280-Pro magnetic stirrer provided by Dlab Scientific Inc., China, was used for stirring and mixing the solution with a speed of 450 RPM for 30 min.

Special porous filter made of stainless steel with three different pore throat sizes of 1  $\mu m$ , 5  $\mu m$  and 10  $\mu m$  was used in this study for  $CO_2$  MB-CGA generation.

The experimental methodology was divided into three main analyses (Fig. 2a). The first analysis focused on  $CO_2$  MB-CGA generation using three different pore size filters. Microbubbles generated from each filter were compared for their diameter size distribution. The stabilization

analysis was performed as well to observe the microbubbles behavior for a certain period of time. The second analysis focused on microbubbles diameter size impact on sweep efficiency, as well as recovery comparison with normal  $CO_2$  gas and polymer and surfactant solution. The third analysis focused on microbubble gas blocking ability to improve the sweep efficiency in heterogeneous porous media. All experiments and analyses were carried out under ambient pressure and room temperature.

### $CO_2$ microbubble colloidal gas aphones generations and analysis

The  $CO_2$  gas was injected through the porous filter into surfactant and polymer solution to create the microbubbles with a constant flow rate of 30 mL/min. (Fig. 2b). Three different pore throat size filters were used to generate different dominant sizes of microbubbles in the solution. The  $CO_2$  MB-CGA from each filter was collected, recorded and analyzed under EVOS XL Core Imaging System Digital Microscope provided by Life Technology Corp., USA. The microbubbles images were stored in digital format for diameter size measurement and analysis with ImageJ ver.1.52a software provided by National Institutes of Health, USA. Three hundred bubbles were selected randomly from the stored digital images for this measurement and analysis. Some random samples were also taken and recorded by digital microscope in every 6 h (for a total of 24 h). Two hundred bubbles were selected

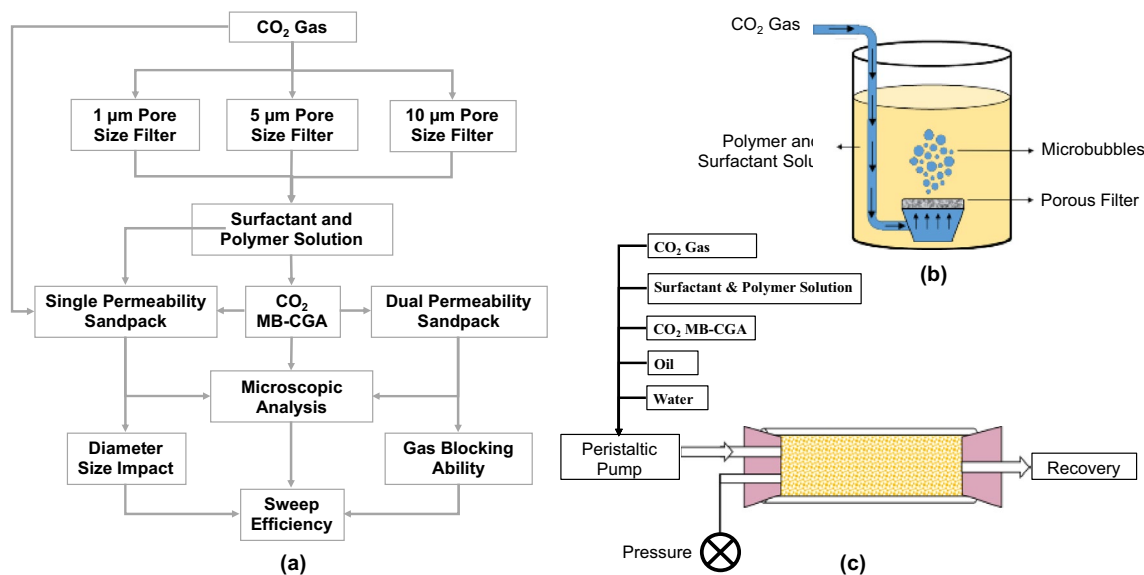


**Fig. 2** a Experimental procedures and analyses, b schematic of  $CO_2$  MB-CGA generation using a porous filter, c schematic of single-permeability sandpack experiment

randomly from each sampling time for the microbubble stabilization analysis.

### CO<sub>2</sub> microbubble diameter size impact on sweep efficiency analysis

The single-permeability sandpack was prepared by filling 120 µm grain size of sands into a glass tube with an inner diameter of 2.5 cm and a length of 25 cm. Each end of the tube was insulated by a rubber cap equipped with in/output flowline for fluid injection and recovery (Fig. 2c). The tube was initially filled with 60 ml of water followed by sands filling. The initial pore volume was calculated by measuring the water volume displacement after filling the sands into tubes. The permeability was calculated using Darcy's law with a flow rate, and the pressure data were obtained from pumping the water into the sandpacks.

The sandpack was next saturated with oil by injecting Japan Light oil. The SJ-1211H peristaltic pump provided by Atto Corp., Japan, was used for the injection process with a constant flow rate of 1.5 mL/min for 2.0 PV (pore volume) of injection volume. The pressures during injection were monitored using GC31-364 pressure gauge provided by Nagano Keiki Co. Ltd., Japan. The fluids recovery was collected every 0.1 PV of injection volume along with pressure reading at that time. The original oil in place (OOIP) inside sandpack and irreducible water were calculated from the initial volume, injected fluid volume and recovery volume. The sandpacks properties are summarized in Table 1.

The next step was water flooding injection with a constant flow rate of 1.5 mL/min for 2.0 PV of injection volume. The fluids recovery was collected with the same method, as well as the pressure recording. These steps were repeated as a preparation of every new sandpack that will be used for tertiary recovery injection with CO<sub>2</sub> MB-CGA generated from three different porous filters, polymer and surfactant solution and CO<sub>2</sub> gas.

The CO<sub>2</sub> MB-CGAs generated from each of the three porous filters were then injected into separate sandpacks with the same constant flow rate of 1.5 mL/min for 2.0 PV of injection volume. The fluids recovery was collected and pressure reading was recorded with the same as the previous procedure for every 0.1 PV of injection volume. The recovery results and recorded pressure were compared each other for the diameter size impact analysis on sweep efficiency.

Fluid recovery was also sampled randomly during the injection process for microscopic observation and analysis. Wet-sand samples were collected directly from sandpack after finishing every CO<sub>2</sub> MB-CGA injection. The samples were taken from each end of the sandpack, as well as from the middle part. These samples were observed under digital microscope for microbubbles behavior and stability analysis.

The same tertiary injection process was carried out with polymer and surfactant solution. The CO<sub>2</sub> gas tertiary recovery experiment was carried out with water alternating gas (WAG) method. The CO<sub>2</sub> gas and water were injected alternately every 0.5 PV of injection volume. The total WAG injection volume was performed for 2.0 PV. The fluid recovery and pressure recording were carried out with the same procedure. The recovery results and recorded pressure were compared with CO<sub>2</sub> MB-CGA results for benchmarking and sweep efficiency analysis.

### Microbubble gas blocking impact on heterogeneous porous media analysis

Two sandpacks with different permeability that connected each other were prepared for this analysis (Fig. 3). The sands with a grain size of 100 µm were used for lower-permeability sandpack and those with a grain size of 150 µm were used for higher-permeability sandpack. The sandpack properties are listed in Table 1. Each sandpack was saturated with oil separately and then to be connected each other in the input flowline for secondary recovery with water flooding and tertiary recovery with CO<sub>2</sub> MB-CGA fluid.

Then, water flooding injection was carried out with a constant flow rate of 1.5 mL/min for 2.0 PV of injection volume. The PV used for this experiment was the total PV of both sandpacks. The fluids recovery from both sandpacks output flowlines was collected in every 0.1 PV of injection volume. The pressure reading was recorded as well.

Based on the single-permeability sandpack experiment, the best CO<sub>2</sub> MB-CGA performance from one of the porous filters was selected. The CO<sub>2</sub> MB-CGA injection was carried out with the same procedure as the previous water flooding. Fluid recovery was sampled randomly during the injection process from both sandpack output flowlines for microscopic observation and analysis. Wet-sand samples were

**Table 1** Sandpack properties prepared for the experiments

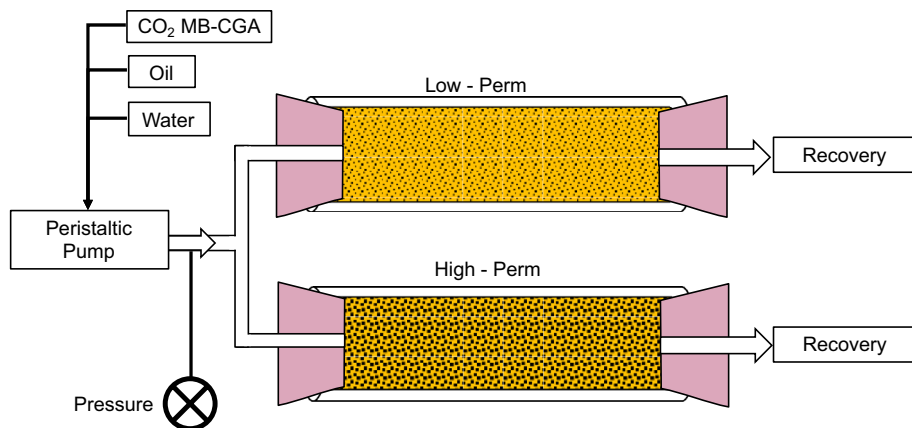
Sandpack	Porosity (%)	Permeability (mD)	Irreducible water (%)	Original oil in place (%)
SP#1	45.22	3500	5.96	94.04
SP#2	43.48	3500	5.40	94.60
SP#3	39.13	4000	3.11	96.89
SP#4	43.48	4000	4.20	95.80
SP#5	41.74	3000	7.71	92.29
LSP <sup>a</sup>	39.13	1200	9.58	90.42
HSP <sup>b</sup>	41.74	4700	2.89	97.11

<sup>a</sup>Low-permeability sandpack

<sup>b</sup>High-permeability sandpack



**Fig. 3** Schematic of dual-permeability sandpack for the heterogeneous porous media experiment



also collected directly from both sandpacks with the same procedure as a single-permeability sandpack experiment. The recovery results from both low-and high-permeability sandpacks were compared each other for sweep efficiency analysis.

## Results and discussion

### CO<sub>2</sub> MB-CGA generation using the porous filter

In general, the three different pore throat size filters were able to generate a wide range of microbubble sizes, from less than 10 μm up to more than 200 μm of microbubble diameter size (Fig. 4a–c).

However, it was observed that each filter generated different distribution dominant sizes of microbubbles. In

observation over 300 random samples of microbubbles generated from each filter, the smaller the pore throat size, the smaller the microbubbles dominant size. The filter with a pore size of 1 μm generated microbubbles with a dominant size of 10–50 μm, while the filter with a pore size of 5 μm and 10 μm generated microbubbles with a dominant size of 40–110 μm and 70–150 μm, respectively (Fig. 4d).

The observation of microbubbles inside the glass tube for 24 h showed that microbubbles were slowly segregated from the solution and sorted by their size (Fig. 5a). The larger sizes were accumulated at the top followed by the medium sizes, while the small sizes were settled at the bottom with the solution. This showed the MB-CGA behavior as gas in liquid-like form that will make a unique flow behavior in porous media.

The size was observed for 200 random samples of microbubbles in every 6 h (a total of 24 h) (Fig. 5d). The

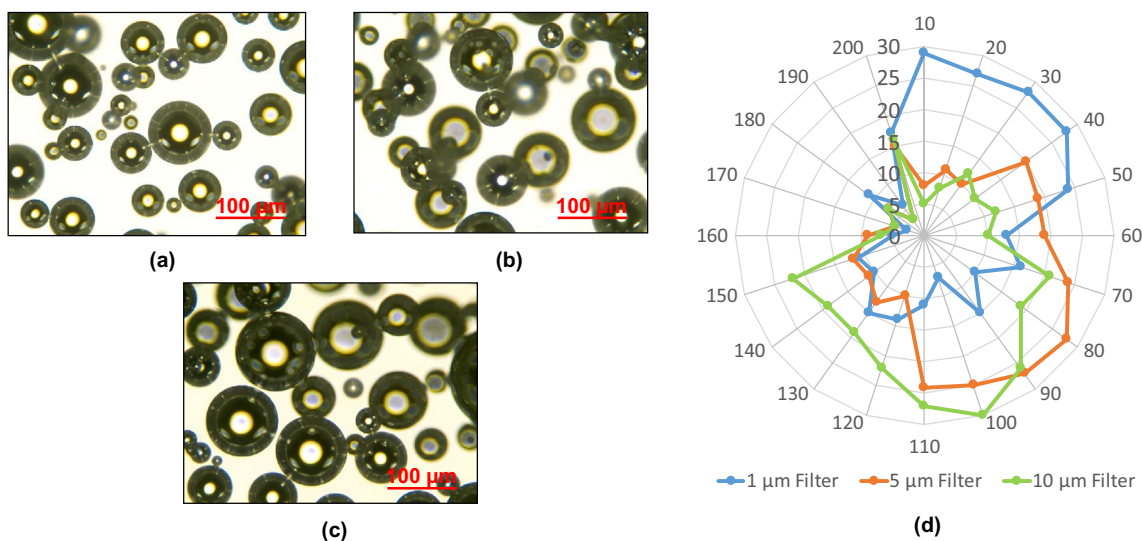


**Fig. 4** Microscopic images of CO<sub>2</sub> MB-CGA generated using a porous filter with a pore throat size of **a** 1 μm, **b** 5 μm, **c** 10 μm and **d** microbubble distribution size from three different pore size filters

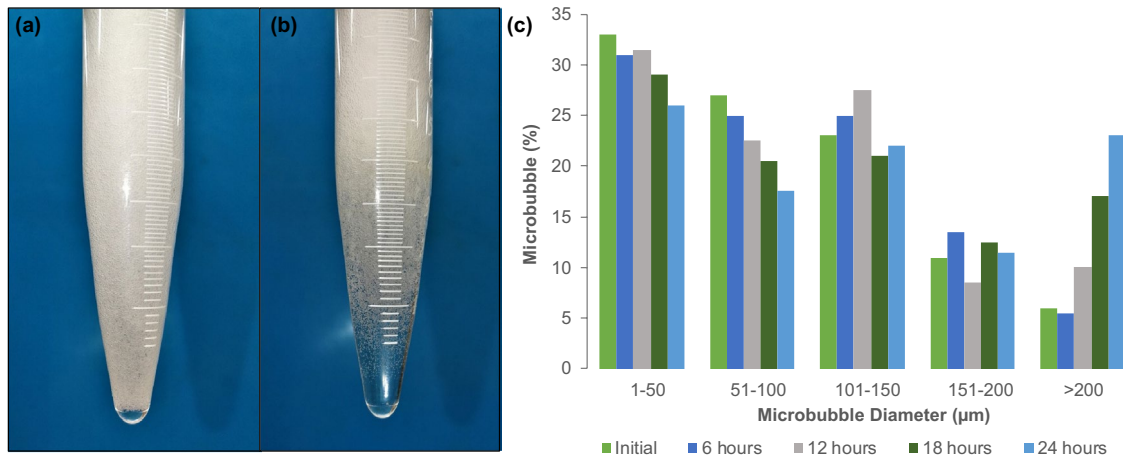


**Fig. 5** Microbubbles observation behavior **a** at an initial hour, **b** after 24 h, **c** microbubble size change for 24 h

microbubble was reduced individually in size by the time. Some initial small-sized microbubbles less than  $10\ \mu\text{m}$  were disappeared and dissolved into solution. Some amount of microbubbles were also merged each other creating larger-sized microbubbles that will bring advantages to gas blocking ability. During observation, it was noted that the agglomerated microbubbles were more stable than individual microbubble (Fig. 6). There was rarely a change in size of these agglomerated microbubbles during 24-h observation. Other author reported that the stability of the agglomerated apheres could reach a period of months (Gupta and Cawiezel 2013).

### CO<sub>2</sub> MB-CGA diameter size impact on sweep efficiency

Following the secondary water flooding recovery, the CO<sub>2</sub> MB-CGA generated by the porous filter with a pore throat size of  $1\ \mu\text{m}$  was injected into sandpack with a constant flow rate of  $1.5\ \text{mL}/\text{min}$  for 2.0 PV of injection volume. The injection rate and volume were following the common core sample flooding method by other previous authors after upscaling to sandpack dimension (Akai et al. 2015; Shi et al. 2016; Sagir et al. 2016; Phukan et al. 2019; Zifar and Pourafshary 2019). These microbubbles with a dominant size of  $10\text{--}50\ \mu\text{m}$  were injected into SP#1 sandpack whose

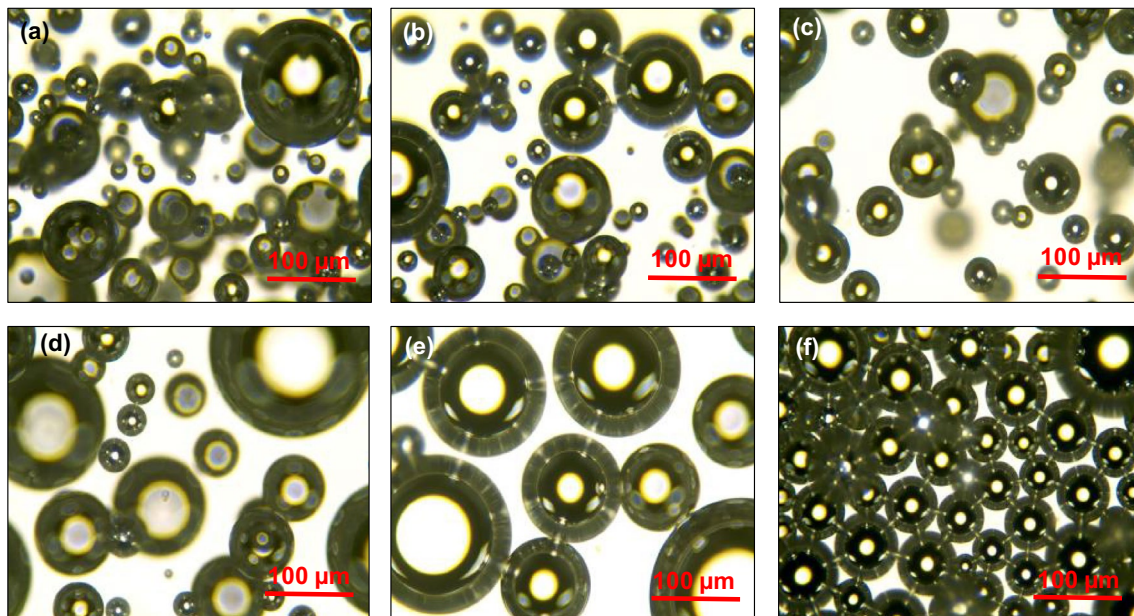


**Fig. 6** Microscopic images of microbubble at **a** an initial hour, **b** 6 h, **c** 12 h, **d** 18 h, **e** 24 h, **f** agglomerated microbubbles

properties were 45.22% of porosity, 3500 mD of permeability, 5.96% of irreducible water and 94.04% of original oil in place. The recovery from this tertiary injection showed additional 26.38% of oil recovery. Previously, the secondary recovery with water flooding already produced 71.78% of oil recovery, causing a total recovery of 98.16% of original oil in place. The maximum pressure reading during the injection process was 124 kPa.

The next injection was carried out using the CO<sub>2</sub> MB-CGA generated by the porous filter whose pore throat size was 5 μm. The microbubbles with a dominant size of 40–110 μm were injected into SP#2 sandpack with the same constant flow rate and volume of previous injection. The sandpack properties were 43.48% of porosity, 3500 mD of permeability, 5.40% of irreducible water and 94.60% of original oil in place. This tertiary recovery gave additional 25.37% of oil recovery with a maximum pressure reading of 133 kPa during the injection process. The total recovery in addition to 70.82% of secondary oil recovery was 96.19% of original oil in place.

Following next was the injection of CO<sub>2</sub> MB-CGA generated by the porous filter whose pore throat size was 10 μm. The microbubbles with a dominant size of 70–150 μm were injected into SP#3 sandpack with the same procedure of previous injections. The sandpack properties were 39.13% of porosity, 4000 mD of permeability, 3.11% of irreducible water and 96.89% of original oil in place. The recovery result showed 21.10% of additional oil recovery. The maximum pressure reading during the injection was 158 kPa. In total, the recovery was 93.12% of original oil in place, in addition to 72.02% of secondary oil recovery with water flooding.

The summarized results of these experiments are given in Table 2, and the visualization graph of these experiments is shown in Fig. 7a. The recovery results showed that the smaller dominant size of 10–50 μm gave more additional oil recovery than larger dominant size of microbubbles up to 5.28% of oil recovery. This showed that microbubbles in smaller sizes played a significant role in increasing the sweep efficiency.

The pressure reading during the CO<sub>2</sub> MB-CGA injection process was gradually increased, indicating that the

MB-CGA was blocking the pores and throats of the porous media (Shi et al. 2016). The maximum pressure reading showed that the dominant larger microbubbles size of 70–150 μm had a higher pressure than others up to 27.5% of injection pressure. This showed that the larger microbubbles size had more advantage in blocking ability. This advantage would divert more fluid to lower permeable zone, increasing the overall sweep efficiency.

For comparison and benchmarking purposes, the tertiary injections were also carried out with the polymer and surfactant solution and CO<sub>2</sub> gas. The same procedures were applied to both experiments. The CO<sub>2</sub> MB-CGA recovered more oil up to 13.29% of additional oil recovery than normal CO<sub>2</sub> gas. It was also observed that the CO<sub>2</sub> gas had earlier breakthrough than any other fluids.

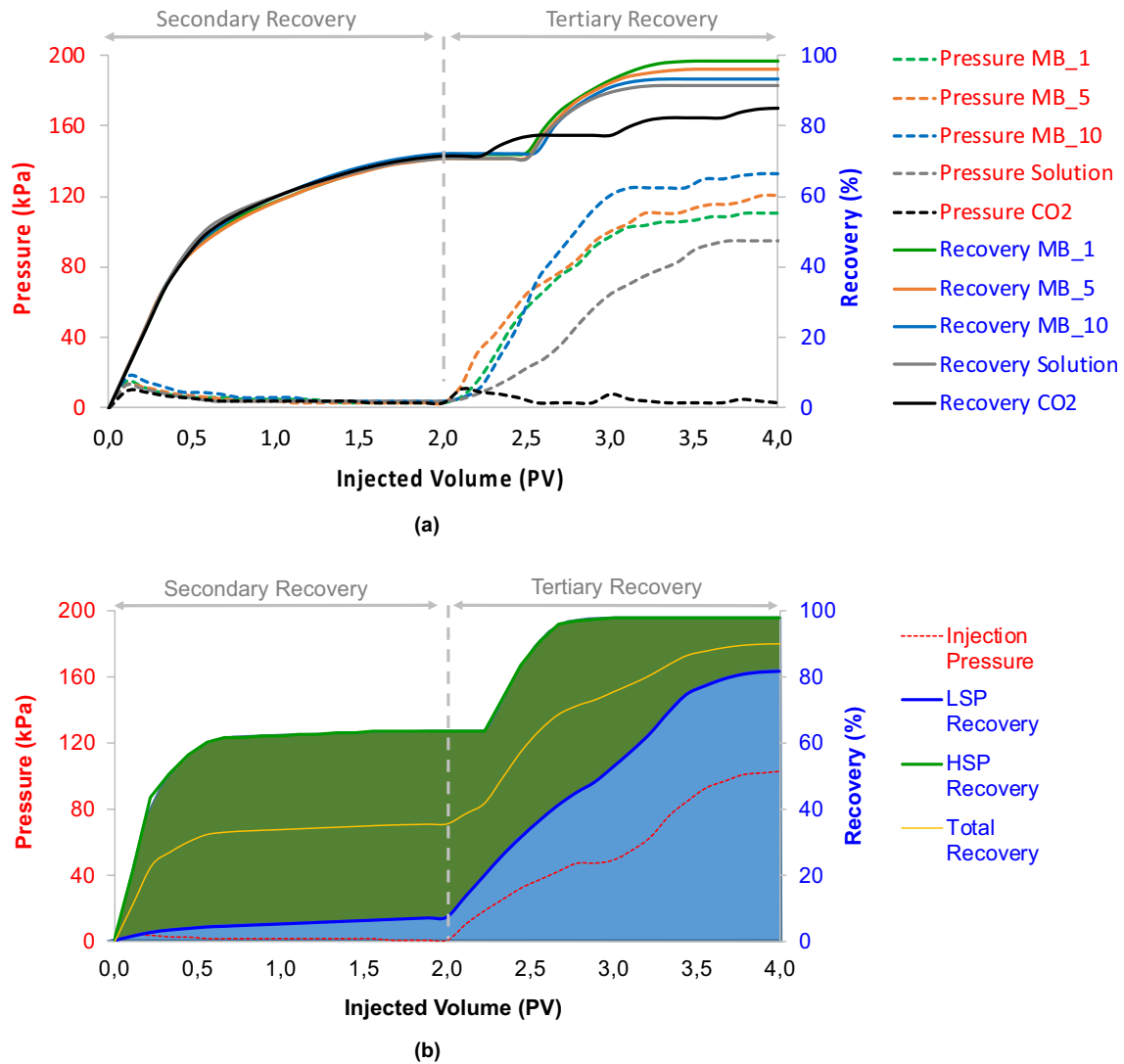
The CO<sub>2</sub> MB-CGA recovered more oil up to 7.59% of oil recovery than polymer and surfactant solution injection. However, it was noticed that CO<sub>2</sub> MB-CGA had earlier breakthrough by 0.1 PV of injection volume. This was expected since the CO<sub>2</sub> MB-CGA contains more gas than the solution, thus higher mobility. The pressure reading showed that CO<sub>2</sub> MB-CGA had more resistance in injection than the polymer and surfactant solution. This showed the gas blocking ability of microbubbles that will divert the fluid flow from the high-permeability zone to the lower-permeability zone, increasing the overall sweep efficiency. However, a dominant larger microbubbles size would not be able to penetrate the smaller pore throat; larger microbubble size tends to block the smaller pore throat earlier that will lead to less sweep efficiency compared with dominant smaller size of microbubbles, hence showing slightly lower recovery in comparison.

Figure 8 shows the microscopic image of some random samples taken during the injection of CO<sub>2</sub> MB-CGA. The samples were collected between 1.0 and 1.5 PV of injection volume where the mixture of water, oil and CO<sub>2</sub> MB-CGA was observed in the output flowline and after 2.0 PV of injection volume where the recovery fluid was dominant of CO<sub>2</sub> MB-CGA fluid. The microbubbles were stable enough to be injected into porous media, they were still present in good shape on the recovery fluids. The numbers of microbubbles in the recovery fluids were less than

**Table 2** The results of sandpack experiments with CO<sub>2</sub> MB-CGA, polymer and surfactant solution and CO<sub>2</sub> gas

Sandpack	Secondary oil recovery (%)	Tertiary oil recovery (%)	Total oil recovery (%)	Maximum pressure (kPa)	Tertiary injection fluid
SP#1	71.78	26.38	98.16	124	CO <sub>2</sub> MB-CGA_1 μm Filter
SP#2	70.82	25.37	96.19	133	CO <sub>2</sub> MB-CGA_5 μm Filter
SP#3	72.02	21.10	93.12	158	CO <sub>2</sub> MB-CGA_10 μm Filter
SP#4	70.77	18.79	89.56	95	Polymer and surfactant solution
SP#5	71.56	13.09	84.65	17	CO <sub>2</sub> gas





**Fig. 7** Recovery and injection pressure; **a** single-permeability sandpack experiments with CO<sub>2</sub> MB-CGA, polymer and surfactant solution, and CO<sub>2</sub> gas, **b** dual-permeability sandpack experiment with water flooding and CO<sub>2</sub> MB-CGA

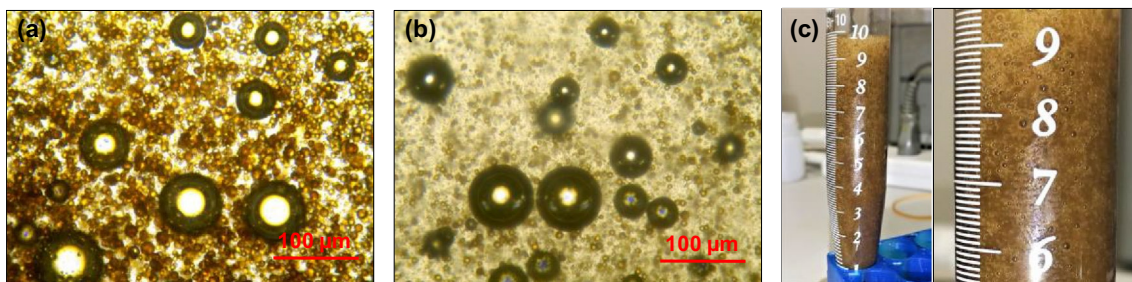


**Fig. 8** Microscopic images of fluid recovery; **a** mixture of water, oil and CO<sub>2</sub> MB-CGA, **b** dominant of CO<sub>2</sub> MB-CGA fluid, **c** fluid recovery samples

the initially injected microbubbles. This is because some microbubbles were dissolved in solution and other fluids,

and some were left behind, trapped inside the porous area and/or blocking the high-permeability zone.



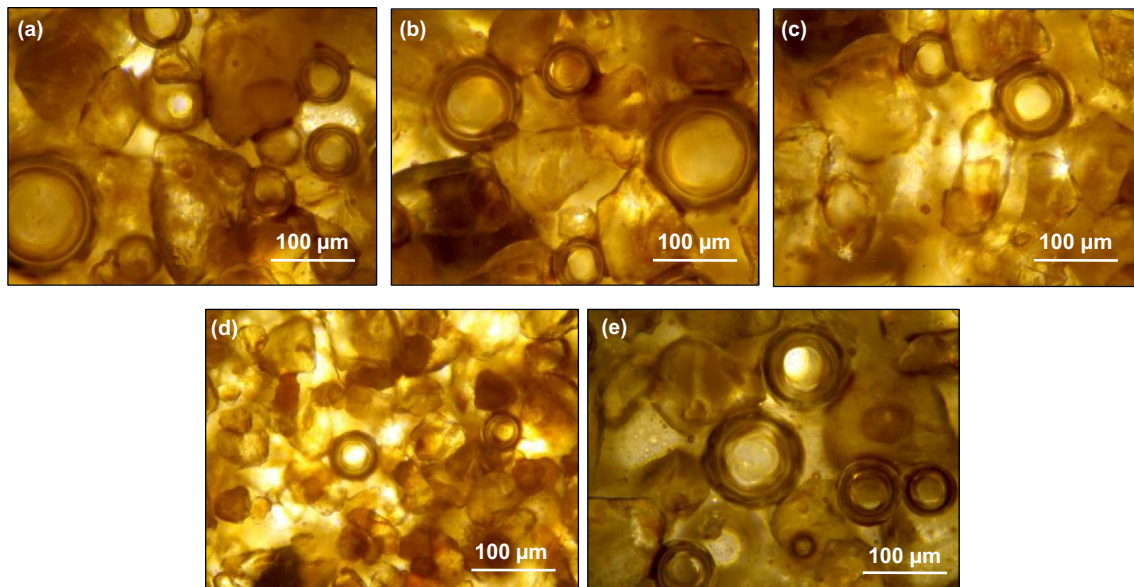


**Fig. 9** Microscopic images of wet-sand samples from single sandpack **a** near input flowline, **b** middle of sandpack, **c** near output flowline and from dual sandpack, **d** LSP, **e** HSP

The wet-sand samples directly taken from the sandpack after CO<sub>2</sub> MB-CGA injection process showed the presence, stability and behavior of microbubbles inside porous media (Fig. 9a–c). The presence of microbubbles was observed in all samples taken near the input flowline, in the middle of sandpack and near the output flowline. This added another proof of microbubbles stability to flow through porous media. It was noticed that the numbers of microbubbles observed were decreased toward the output flowline, mostly due to microbubbles dissolution into fluids. From the microscopic images of wet-sand samples, it was also observed how microbubbles block mechanism inside porous media with single bubble blocking, agglomerated blocking and squeezed microbubbles (Fig. 10).

### CO<sub>2</sub> MB-CGA gas blocking impact on heterogeneous porous media

The low- and high-permeability sandpacks were prepared for this experiment and analysis. The low-permeability sandpack (LSP) with 1700 mD of permeability and the high-permeability sandpack (HSP) with 4700 mD of permeability were connected in the input flowline for the secondary recovery with water flooding followed by tertiary recovery with CO<sub>2</sub> MB-CGA generated with a 1-µm pore size filter. The results of these experiments are summarized in Table 3 and shown in Fig. 7b.

The secondary recovery experiment with water flooding showed that most of the injected water volumes were flowed into higher-permeability sandpack. This caused big difference in oil recovery between low-permeability sandpack and high-permeability sandpack. The recovery from the high-permeability sandpack was 63.62% of original oil in place, while the low-permeability sandpack was recovered

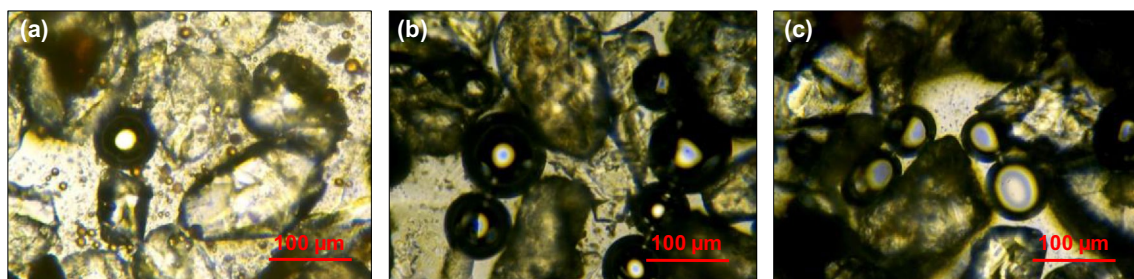


**Fig. 10** Microscopic images of microbubbles inside sand pores; **a** single blocking, **b** agglomerated blocking, **c** squeezed microbubbles

**Table 3** The results of dual-permeability sandpacks experiments

Sandpack	Secondary oil recovery (%)	Tertiary oil recovery (%)	Total oil recovery (%)	Maximum pressure (kPa)	Tertiary injection fluids
LSP <sup>a</sup>	7.14	74.65	81.80	103	CO <sub>2</sub> MB-CGA_1 μm Ffilter
HSP <sup>b</sup>	63.62	34.10	97.71	103	CO <sub>2</sub> MB-CGA_1 μm filter

<sup>a</sup>Low-permeability sandpack<sup>b</sup>High-permeability sandpack

only 7.14% of original oil in place. The injection pressure was almost flat throughout the water flooding experiment.

The tertiary recovery experiment with CO<sub>2</sub> MB-CGA fluid showed the improvement in low-permeability sandpack recovery but and maintenance of the optimum recovery in the high-permeability sandpack as well. The recovery results from this tertiary injection showed additional 74.65% of oil recovery from the low-permeability sandpack. Adding to the secondary recovery result, the total recovery of the low-permeability sandpack was 81.80% of original oil in place. The tertiary recovery result from the high-permeability sandpack showed additional 34.10% of oil recovery that made the total recovery from the high-permeability sandpack become 97.71% of original oil in place. The total recovery from this heterogeneous porous media sandpack experiment was 89.78% of original oil in place.

The change in recovery volume ratio between low-permeability sandpack and high-permeability sandpack during secondary recovery and tertiary recovery showed obvious change in flow volume pattern distribution. During water flooding in secondary recovery experiment, most of the injected fluid was flowed dominantly through high-permeability sandpack. The recovery volume ratio between low-permeability sandpack and high-permeability sandpack was 1:57. During the CO<sub>2</sub> MB-CGA injection, the recovery volume ratio between low-permeability sandpack and high-permeability sandpack was increased to 1:4. This showed that microbubble gas blocking ability was effective in diverting some of the injection fluid volume from dominantly flowed through high-permeability zone into lower-permeability zone.

It was noticed that the injection pressure was started to gradually increase as soon as the CO<sub>2</sub> MB-CGA was injected. At the same time, the recovery from the low-permeability sandpack was gradually increased as well. This showed that the microbubble gas blocking ability was started as soon as they entered the porous media.

The wet-sand samples were also collected from near output flowline on both sandpacks (Fig. 9d, e). It was observed that the number of microbubbles in the low-permeability sandpack was less than in high-permeability sandpack. The dominant sizes observed were also different; dominant larger microbubbles were found in higher-permeability sandpack and smaller microbubbles were observed in low-permeability sandpack. This showed that smaller microbubbles had more advantage in

sweeping the lower-permeability zone. The smaller microbubbles were flowed easier through the smaller permeable flow path than the larger size microbubbles.

## Conclusions

Microbubbles with their unique characters offer some advantages that can be utilized in the EOR application. This study aimed to generate different sizes of CO<sub>2</sub> microbubble colloidal gas aphrons using a porous filter with different pore throat sizes, analyze the diameter size impact on sweep efficiency and investigate microbubble gas blocking impact on sweep efficiency in heterogeneous porous media. The summary results are as follows:

- Microbubbles with a dominant size of 10–50 μm were generated using 1 μm pore throat size of porous filter, while microbubbles with a dominant size of 40–110 μm and 70–150 μm were generated using 5 μm and 10 μm pore throat size of porous filters, respectively.
- Microbubbles with a dominant size of 10–50 μm gave more additional oil recovery up to 5.28% difference compared with a larger dominant size of microbubbles, showing the advantage of smaller microbubbles in increasing the area of sweep efficiency.
- Microbubbles with a dominant size of 70–150 μm showed 27.5% of higher injection pressure than a smaller dominant size of microbubbles, showing their advantage in gas blocking ability and diverting the fluid flow pattern from dominantly flowed in high-permeability into lower-permeability zone.
- CO<sub>2</sub> MB-CGA tertiary recovery injection showed additional recovery up to 26.38% of original oil in place, showing its advantages over CO<sub>2</sub> gas injection with 13.09% additional oil recovery and surfactant and polymer injection with 18.79% additional oil recovery.
- During the heterogeneous porous media experiment, the recovery volume ratio between low-permeability sandpack and high-permeability sandpack was increased from 1:57 during water flooding to 1:4 during the CO<sub>2</sub> MB-CGA injection. This showed the effective of microbubble gas blocking ability in blocking the majority of high-permeability path flow and divert-

ing the fluid flow from dominantly flowed through the high-permeability zone in more evenly distributed fluid flow in the lower-permeability zone.

- CO<sub>2</sub> MB-CGA injection in heterogeneous porous media showed the improvement in sweeping efficiency in the low-permeability zone with additional 74.65% of oil recovery from only 7.14% of water flooding secondary recovery result.

Both small- and large-sized microbubbles had their own advantages in increasing the sweep efficiency. The smaller microbubbles have more surface contact area and will be able to flow through smaller throat of low-permeability zone, thus increasing the area of sweep efficiency. The larger microbubbles will be able to block more of the high-permeability path flow and will divert more fluids to the lower-permeability zone, hence increasing the sweep efficiency as well.

An adequate, proportional and well-distributed number of small- and large-sized microbubbles will maximize the advantages of microbubbles for increasing the overall sweep efficiency, especially in the heterogeneous porous media or reservoir.

**Acknowledgements** The authors gratefully acknowledge Kyushu University and Japan Student Services Organization (JASSO) for the financial support during the research.

**Open Access** This article is distributed under the terms of the Creative Commons Attribution 4.0 International License (<http://creativecommons.org/licenses/by/4.0/>), which permits unrestricted use, distribution, and reproduction in any medium, provided you give appropriate credit to the original author(s) and the source, provide a link to the Creative Commons license, and indicate if changes were made.

## References

- Akai T, Xue Z, Yashamita Y, Yoshizawa M (2015) Application of CO<sub>2</sub> microbubble for the innovative CO<sub>2</sub>-EOR. SPE-177672-MS. Presented at the Abu Dhabi international petroleum exhibition and conference, Abu Dhabi, 9–12 Nov 2015
- Bjorndalen N, Alvarez JM, Jossy E, Kuru E (2011) A study of the effects of colloidal gas aphron composition on pore blocking. SPE-121417-PA. SPE drilling and completion 26
- Blunt M, Fayers FJ, Orr FM Jr (1993) Carbon dioxide in enhanced oil recovery. *Energy Convers Manag* 34:1197–1204
- Ghedan S (2009) Global laboratory experience of CO<sub>2</sub>-EOR flooding. SPE-125581-MS. Presented at the SPE/EAGE Reservoir

- characterization and simulation conference, Abu Dhabi, UAE, 19–21 Oct 2009
- Ghosh M (2013) Laboratory study on the generation and characterization of CO<sub>2</sub> colloidal gas aphrons. University of Alberta, Canada
- Growcock FB (2005) Enhanced wellbore stabilization and reservoir productivity with aphron drilling fluid technology. *GTI-05/0226. GasTIPS* 11:12–16
- Gupta S, Cawiezel KE (2013) Method of fracturing with aphron containing fluids. Patent 0126163 A1, USA
- Hiramoto H, Kuku K, Kurihara M, Akai T, Takakuwa Y, Sato K, Tsuchiya Y, Araki N, Shirai S (2016) Experiments of microbubble CO<sub>2</sub> EOR using Berea sandstone core samples. Presented at the 22nd formation evaluation symposium, Japan, Sept 29–30 2016
- Holm LW, Josendal VA (1974) Mechanisms of oil displacement by carbon dioxide. SPE-4736-PA. *J Petrol Technol* 26(12):1427–1438
- Lake LW (1989) Enhanced oil recovery. Prentice-Hall Inc, Englewood Cliffs
- Longe TA (1989) Colloidal gas aphrons: generation, flow characterization and application in soil and groundwater decontamination. Ph.D. dissertation, Virginia Polytechnic Institute and State University, USA
- Phukan R, Gogoi SB, Tiwari P (2019) Enhanced oil recovery by alkaline-surfactant-alternated-gas/CO<sub>2</sub> flooding. *J Petrol Explor Prod Technol* 9:247–260
- Rogers J D and Grigg RB (2000) A literature analysis of the WAG injectivity abnormalities in the CO<sub>2</sub> process. SPE-59329-MS. Presented at the SPE/DOE improved oil recovery symposium, Tulsa, Oklahoma, 3–5 Apr 2000
- Sagir M, Tan IM, Mushtaq M, Pervaiz M, Tahir MS, Shahzad K (2016) CO<sub>2</sub> mobility control using CO<sub>2</sub> philic surfactant for enhanced oil recovery. *J Petrol Explor Prod Technol* 6:401–407
- Sebba F (1987) Foams and biliquid foams-aphrons. Wiley, Chichester
- Shi S, Wang Y, Li Z, Chen Q, Zhenghao Z (2016) Laboratory investigation of the factors impact on bubble size, pore blocking and enhanced oil recovery with aqueous colloidal gas aphron. *J Petrol Explor Product Technol* 6:409–417
- Stalkup FI Jr (1978) Carbon dioxide miscible flooding: past, present, and outlook for the future. SPE 7042. Presented at the 5th symposium on improved methods for oil recovery, Tulsa, Oklahoma
- Telmadarre A, Doda A, Trivedi JJ, Kuru E, Choi P (2016) CO<sub>2</sub> microbubbles—a potential fluid for enhanced oil recovery: bulk and porous media studies. *J Petrol Sci Eng* 138:160–173
- Xue Z, Yamada T, Matsuoka T, Kameyama H, Nishio S (2011) Carbon dioxide microbubble injection—enhanced dissolution in geological sequestration. *Energy Procedia* 4:4307–4313
- Zifar D, Pourafshary P (2019) A new approach for predicting oil recovery factor during immiscible CO<sub>2</sub> flooding in sandstones using dimensionless numbers. *J Petrol Explor Prod Technol*. <https://doi.org/10.1007/s13202-019-0630-0>

**Publisher's Note** Springer Nature remains neutral with regard to jurisdictional claims in published maps and institutional affiliations.